# Structure and Ionic Conductive Properties of Polydioxolane–Polyurethane-Based Electrolytes

**WEIHUA ZHU,[1] BING YANG,[1] XINLING WANG,[1] LEI WANG,[1] XIAOZHEN TANG,[1] CHANGZHENG YANG[2]**

[1] School of Chemistry and Chemical Technology, Shanghai Jiao Tong University, Shanghai 200240, People's Republic of China

[2] School of Chemistry and Chemical Engineering, Nanjing University, Nanjing 210008, People's Republic of China

**ABSTRACT:** A series of polyurethanes (PUs) with different polyether soft segments [polydioxolane (PDXL), polyethylene glycol (PEG), or PDXL/PEG] were synthesized successfully, and solid polymer electrolytes based on PU/LiClO$_4$ complexes were prepared. The relations between structure and the ionic conductive properties of the PU-based electrolytes were investigated by means of Fourier transform infrared spectroscopy, differential scanning calorimetry, dynamic mechanical analysis, and complex impedance analysis. Results showed that the glass-transition temperature ($T_g$) of PDXL–PU was lower than that of PEG–PU. Doped lithium perchlorate (LiClO$_4$) salt could be dissolved well in soft segments of PDXL–PU. The ionic conductivity of the PDXL–PU/LiClO$_4$ complex could reach a value of $2 \times 10^{-5}$ S/cm at room temperature without the addition of an organic plasticizer. The system with PDXL/PEG as a soft segment had a higher $T_g$ and a lower ionic conductivity than the one with PDXL as a soft segment. © 2002 John Wiley & Sons, Inc. J Appl Polym Sci 83: 103–111, 2002

**Key words:** polydioxolane; polyurethanes; ionic conductivity; glass transition; solid polymer electrolyte; structure–property relations

## INTRODUCTION

Since Wright[1] reported that the complexes of polyethylene oxide (PEO) and lithium salts showed good ionic conductivity at room temperature, the study of solid ionic conductive polymers has blossomed.[2] In recent years, solid polymer electrolytes (SPEs) have attracted a great deal of scientific interest due to their potential applications, including high-energy-density batteries, electrochromic devices, chemical sensors, and smart windows.[3] Particularly, rechargeable lithium batteries that can supply over 3 V from a single unit cell are important for driving large-scale integration or related devices such as liquid-crystal displays and electrochromic displays.[4]

PEO/lithium salt complexes have been extensively studied in high-temperature applications, but their low ionic conductivity and poor mechanical properties below 65°C due to their amorphous-to-crystalline phase transition have hindered their use in room-temperature applications.[5–7] Therefore, many researchers have focused their attention on modifying the structure of PEO or developing new SPE systems containing ether groups.[8–13] Alamgir and others[14,15] reported that a complex of polydioxolane (PDXL) and lithium salt was amorphous at room temperature and exhibited an ionic conductivity of $10^{-6}$ to $10^{-5}$ S/cm at a [O]/[Li] (molar ratio) of 8–16.
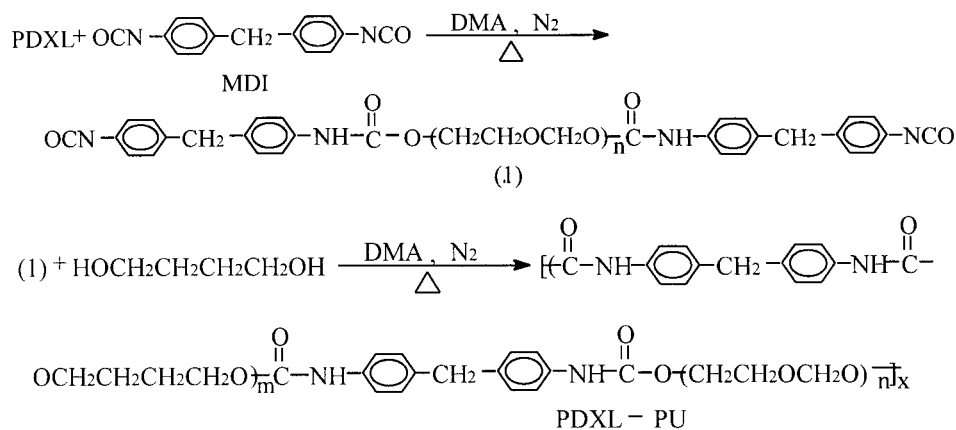
**Scheme 1**

Therefore, PDXL might be a better host polymer than PEO. However, the previous study[15] also showed that the PDXL-based complex membrane exhibited very poor mechanical properties and was very difficult to prepare, even when the average molecular weight of PDXL reached 43,000.

In this study, PDXL with an average molecular weight of 1000 was incorporated into polyurethane (PU) as a soft segment. The microphase-separated structure of PU could effectively compensate for the drawbacks of PDXL, provide a continuous ionic transport path in the PDXL phase, and give the material excellent structural properties. Hence, PDXL–PU might be a good material that could be used in the field of SPEs.

## EXPERIMENTAL

### Materials

Diphenylmethane-4,4′-diisocyanate (MDI; Aldrich Chemical Co., Milwaukee, WI) was degassed and purified by vacuum distillation. The dopant salt lithium perchlorate (LiClO$_4$; analytical reagent grade; Shanghai Chemical Reagent Factory, Shanghai, China), polyethylene glycol [PEG; number-average molecular weight ($M_n$) = 1000; Aldrich], poly-tetrahydrofuran (PTMO; $M_n$ = 1000; Aldrich), and PDXL ($M_n$ = 880; Aldrich) were dried at 60°C in a vacuum oven for 72 h before use. We dried 1,4-Butanediol (BD; Riedel-de Haën Co., Leicestershire, UK) by refluxing over CaH$_2$ for 4 h to exclude trace water, and then, we distilled it under vacuum. The solvent N,N′-dimethylacetamide (DMA; Shanghai Solvent Factory, Shanghai, China) was dried and distilled before use.

### Preparation of PU

Based on a 1 : 3 : 2 molar ratio of polyether : MDI : BD, several segmented polyether–PUs with different polyether soft segments (PDXL, PEG, PTMO, or PDXL/PEG) used as the matrix polymer in this study were prepared by a typical two-step condensation reaction. The reaction procedure is outlined in Scheme 1.

The segmented PU was synthesized under a nitrogen atmosphere, and 0.15 wt % dibutyltin dilaurate was used as a catalyst. A solution of PDXL in DMA was added dropwise to a solution of MDI in DMA at 40°C. The mixture was stirred at 70°C for 4 h. Then, the temperature was decreased to 40°C, and BD (solvated in DMA) was added into the reacting liquid within 0.5 h. To ensure a complete reaction, the mixture was stirred at 75°C for an additional 2 h. Then, the polymer solution was precipitated into a large amount of distilled water. After filtration, the deposition was put into alcohol for 24 h. The material obtained was dried in a vacuum-drying oven at 60°C for at least 48 h.

Another series of PUs were prepared according to a 1 : 2 : 1 molar ratio of polyether : MDI : BD.

### Preparation of SPE Film

Films of polyether–PU/LiClO$_4$ were prepared with a solution-cast technique. The typical procedure was carried out through dissolution of the appropriate amount of the polyether–PU and LiClO$_4$ in DMA solvent; the resultant solution was then poured into a Teflon plate. After the solvent was evaporated at 60°C in an oven for 24 h, the films were transferred to a vacuum oven

**Table I    Characteristic Bands and Assignments for PDXL–PU IR Spectra**

| Wavenumber (cm$^{-1}$) | Relative Intensity | Assignment | Group |
|---|---|---|---|
| 3334 | Strong | $\nu$(N—H) | Amino group |
| 1729 | Very strong | $\nu$(C=O) | Carbonyl (nonbonded) |
| 1703 | Very strong | $\nu$(C=O) | Carbonyl (bonded) |
| 1598 | Strong | $\nu$(C=C) | Aromatic ring |
| 1413 | Strong | $\nu$(C—C) | Aromatic ring |
| 1110 | Very strong | $\nu$(C—O—C) | Ether group |

and further dried at 70°C for 48 h to remove the residual solvent.

## Measurements

IR spectra were recorded on a Nicolet (United States) 170 SX Fourier transform infrared (FTIR) spectrophotometer at a resolution of 2 cm$^{-1}$. Samples for IR survey were prepared by solution casting on a NaCl plate and dried at 70°C in a vacuum oven for 48 h. The thermograms of PU electrolytes were recorded with a differential scanning calorimeter (PerkinElmer DSC-2C, United States) over a temperature range of −120 to 200°C at a heating rate of 20°C/min. Dynamic mechanical analysis was carried out on a Rheovibron DDVII-C dynamic viscoelastometer (Toyo Baldwin Co., Japan) in a temperature range of 150–200°C, the frequency used was 110 Hz, and the rate was 2°C/min. The frequency of sample collection was 0.5°C. Ionic conductivity measurements with alternating current were conducted on a 378 Electrochemical Impedance System (EG & G Princeton Applied Research, United States) in a frequency range of 10 Hz–10 MHz and a temperature range from room temperature to 120°C. The electrolyte films were cut to a required size and were sandwiched between two silver electrodes. When measured, the cell was kept in a temperature-controlled dry box, and the conductivity was tested at each temperature after equilibration for 30 min.

The ionic conductivity of the samples was calculated by the following equation:

$$\sigma = (1/R_B)d/S \qquad (1)$$

where $\sigma$ is the ionic conductivity, $d$ is the thickness of the sample, $S$ is the area of the Ag electrode, and $R_B$ is the bulk resistance of the sample.

## RESULTS AND DISCUSSION

### Composition of Samples

In this study, PDXL–PU means PU with only PDXL as a soft segment, whereas PEG–PU is PU with PEG as a soft segment. The sample marked PDXL–PEG–PU-16 1 : 2 was a PU/LiClO$_4$ complex with PDXL and PEG (PDXL : PEG 1 : 2) as the soft segment; 16 was the molar ratio of [O]/[Li]. So were the other samples.

### Structure of PUs

Characteristic bands and assignments for PDXL–PU IR spectra are listed in Table I. According to previous studies,[3,16] the strong band at 1110 cm$^{-1}$ is attributed to the C—O—C stretch in the soft segment of PU, whereas the two bands at 1729 and 1703 cm$^{-1}$ are attributed to carbonyl groups in different hard-segment environments of PU. An amino group located in the hard segment could bond with a carbonyl group to form a hydrogen bond so that information for microphase separation could be obtained from a comparison between spectra of hydrogen-bonded carbonyl groups and that of unbonded carbonyl groups.

When the carbonyl spectral region of PDXL–PU was compared, it could be found that in the carbonyl spectral region of PDXL–PEG–PU 1 : 1 (Fig. 1), a fraction of the band corresponding to a hydrogen-bonded carbonyl at about 1703 cm$^{-1}$ decreased, whereas that corresponding to a nonbonded carbonyl at about 1729 cm$^{-1}$ increased. This meant that after the incorporation of PEG into the soft segment, the hydrogen bonding in the hard-segment domains decreased and the number of hard segments entering domains of soft segments increased, which led to the dissociation of short-range ordering in the hard domains of PU elastomers. As a result, compatibility between hard and soft segments was improved.
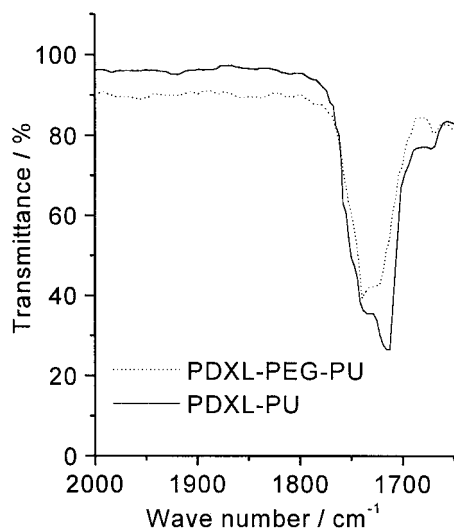
**Figure 1** IR spectra of the carbonyl region of PDXL–PU and PDXL–PEG PU 1 : 1.

Differential scanning calorimetry (DSC) thermograms of the 1 : 2 : 1 series are shown in Figure 2, and DSC data are listed in Table II. In the DSC curve of PDXL–PU, there was an obvious exothermic peak at −29 to 5°C and an endothermic peak at 5–28°C. This indicates that the soft segments crystallized around −29 to 5°C, whereas the crystalline structure was destroyed when the temperature further increased. For PU with PDXL and PEG as soft segments, no endothermic peak was found in the DSC curve. This was due to a loss of long-range ordering induced by the incorporation of PEG into the soft segment. Consequently, the crystallinity of the soft segment was suppressed. More-

over, DSC data also showed that the glass-transition temperature $(T_g)$ of the samples increased with the incorporation of PEG, which was consistent with the results of IR spectra mentioned previously. When PEG was introduced into the soft segment along with PDXL, the number of hard segments entering domains of soft segments increased, which led to a reduction of the mobility of the soft segments and an improvement of the compatibility between hard and soft segments. All these resulted in an increase in the $T_g$ of the soft segment.

Figure 3 shows the DSC thermograms of the 1 : 3 : 2 series, and Table III lists the data obtained from the DSC curves. There was no endothermic peak in the DSC curves of the 1 : 3 : 2 series, which indicates that the soft segment was difficult to crystallize with an increasing content of hard segment. Moreover, it was found that the $T_g$ of the soft segment in the 1 : 3 : 2 series increased and the $T_g$ range became broader with the incorporation of the PEG segment. In addition, the $T_g$ increased gradually with increasing PEG content. This indicates that PEG was compatible with PDXL and that the introduction of PEG into this system could improve the phase compatibility between hard and soft segments. Results also showed that the $T_g$ of PDXL–PU was 20°C lower than that of PEG–PU and similar to that of PTMO–PU, which indicates that the soft segment of PDXL–PU had good flexibility.

We suggested previously that the soft segment of PDXL–PU possessed high ether group density and exhibited good flexibility so that PDXL–PU could be used as an excellent host polymer in the
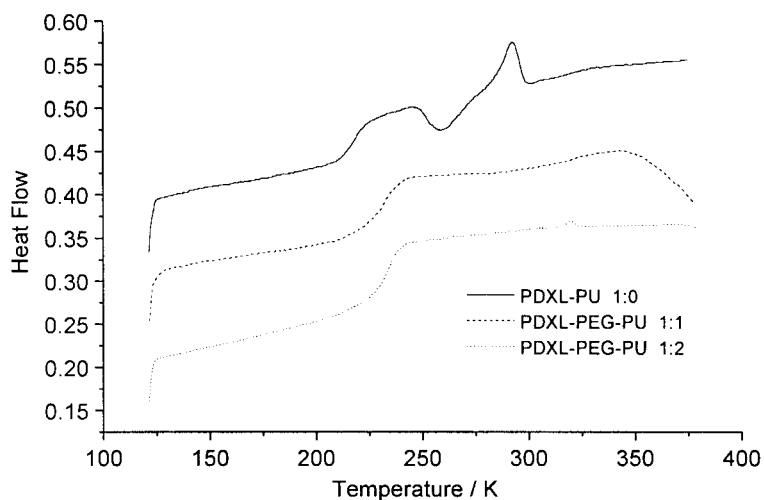


**Figure 2** DSC thermograms of the 1 : 2 : 1 series.

**Table II   DSC Data of the 1 : 2 : 1 Series**

| Sample | $T_g$ (K) | | | $\Delta Heat$ Capacity (Cal/g deg) |
| --- | --- | --- | --- | --- |
| | Onset | Midpoint | $\Delta T$ | |
| PDXL–PU | 213.7 | 218.8 | 28.6 | 0.118 |
| PDXL–PEG–PU 1 : 1 | 223.9 | 232.3 | 39.1 | 0.173 |
| PDXL–PEG–PU 1 : 2 | 225.9 | 233.3 | 43.1 | 0.195 |

field of SPEs. When PEG was incorporated into the 1 : 2 : 1 system as a soft segment, the ordered structure of the PDXL segment was destroyed, and an amorphous domain of the soft segment was obtained, whereas incorporation of PEG into the 1 : 3 : 2 system led to an improvement in compatibility between the hard and soft segments, thus resulting in a less pure soft phase (with a higher $T_g$).[17]

**Structure of Polyurethane/LiClO₄ Complexes**

As shown in the DSC curves of the PDXL–PU/LiClO$_4$ complex series (Fig. 4), wide endothermic peaks were evident above 30°C, which could be due to the fact that LiClO$_4$ interacted with the ether group of PDXL to form a complex and this complex was destroyed at temperatures above 30°C. The thermal transition data (Table IV) showed that with the adulteration of LiClO$_4$, the $T_g$ of samples decreased, and the glass-transition region became broader.

When doped LiClO$_4$ salt was introduced into PEG–PU system, the $T_g$ of the samples shifted to a region of higher temperature, and the glass-transition region became broader, as illustrated in Figure 5 and Table IV. Similar results were obtained for the PEG–PDXL–PU/LiClO$_4$ complex. This was consistent with another investigation of LiClO$_4$-doped PUs containing PTMO as the soft segment.[16] It was suggested that for samples with PEG soft segments, the phase compatibility between hard and soft segments was improved with the introduction of LiClO$_4$ into the system; on the other hand, complexes formed in this system also hindered the motion of the PEG segment, which led to an increase in the $T_g$ of the soft segment.

The dynamic mechanical thermal analysis spectrum of PDXL–PU (Fig. 6) indicates a typical character of two phases, which was due to the existence of microphases of both soft segments and hard segments in the bulk. There was a peak at $-43.2$°C in the loss modulus ($E''$) $-$ temperature ($T$) curve, which was attributed to the glass transition of the soft-segment phase, and an abrupt decrease was found in the storage modulus ($E'$) $-$ temperature ($T$) curve correspondingly.
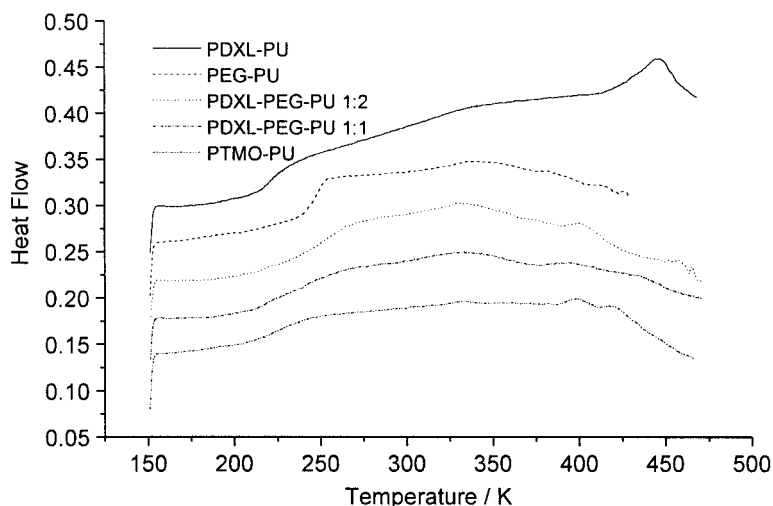


**Figure 3**   DSC thermograms of the 1 : 3 : 2 series.

**Table III    DSC Data of the 1 : 3 : 2 Series**

| | $T_g$ (K) | | | |
|---|---|---|---|---|
| Sample | Onset | Midpoint | $\Delta T$ | $\Delta C_p$ (Cal/g deg) |
| PDXL–PU | 213.7 | 221.4 | 71.1 | 0.092 |
| PDXL–PEG–PU 1 : 1 | 218.5 | 228.2 | 88.6 | 0.123 |
| PDXL–PEG–PU 1 : 2 | 233.8 | 244.3 | 83.6 | 0.124 |
| PEG–PU | 239.2 | 246.0 | 65.1 | 0.142 |
| PTMO–PU | 211.5 | 226.6 | 84.8 | 0.088 |

In addition, incomplete rubbery plateau zones could be seen in the storage modulus $(E')$ − temperature $(T)$ curves. As shown in Figure 6, for all the PDXL–PU/LiClO$_4$ samples, the $T_g$ of the soft-segment phase shifted to a range of lower temperature (below −43.2°C), and this result was consistent with that of DSC mentioned previously.

### Ionic Conductive Properties of Polyurethane/LiClO$_4$ Complexes

Figures 7 and 8 illustrate the concentration dependencies of the ionic conductivity for the PDXL–PU/LiClO$_4$ and PDXL–PEG–PU/LiClO$_4$ series. The results of complex impedance spectra (Fig. 7) show that all the complexes based on PDXL–PU exhibited high ionic conductivities, which reached values of $2 \times 10^{-5}$ S/cm at room temperature and $10^{-4}$ S/cm at 70°C. In contrast, the ionic conductivities of samples with PEG as part of the soft segment were low, as shown in Figure 8. It was clear that the higher the content of PEG was, the lower ionic conductivity was.

Generally speaking, many factors had influence over the ionic conductive properties of SPEs. For the PDXL–PU/LiClO$_4$ system investigated, besides the high density of the coordinating group (C—O—C) and low $T_g$ of PDXL, the amorphous phase of the soft segment should be a significant factor. According to previous studies,[18–20] it was assumed that the charge carries mainly transported in the amorphous phase and the ionic conductivity of polymer/salt complex was predominantly due to the amorphous section of the complex. The previous DSC analysis of the PDXL–PU/LiClO$_4$ series showed that the soft-segment phase of the system was amorphous, which provided the ion transport path and lead to a high ionic conductivity.

Moreover, the concentration of LiClO$_4$ had a great influence on the ionic conductivity of samples. As shown in Figure 7, the sample with a [O]/[Li] of 12 had the highest ionic conductivity, whereas samples with a [O]/[Li] of higher or lower than 12 all exhibited low ionic conductivities.
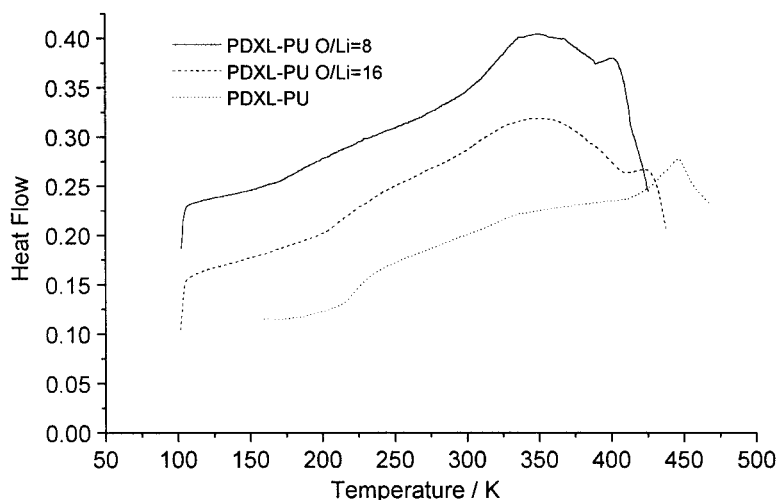


**Figure 4**    DSC thermograms of the PDXL–PU and PDXL–PU/LiClO$_4$ samples.

**Table IV    DSC Data of the PU/LiClO$_4$ Complexes**

| | $T_g$ (K) | | | |
| --- | --- | --- | --- | --- |
| Sample | Onset | Midpoint | $\Delta T$ | $\Delta C_p$ (Cal/g deg) |
| PDXL–PU-0 | 213.7 | 221.4 | 71.1 | 0.092 |
| PDXL–PU-8 | 193.2 | 206.7 | 96.9 | 0.062 |
| PDXL–PU-16 | 203.1 | 213.8 | 73.8 | 0.045 |
| PEG–PU-0 | 239.2 | 246.0 | 65.1 | 0.142 |
| PEG–PU-16 | 249.9 | 258.1 | 88.4 | 0.160 |
| PDXL–PEG–PU-0 1 : 2 | 233.8 | 244.3 | 83.6 | 0.124 |
| PDXL–PEG–PU-16 1 : 2 | 253.8 | 264.7 | 98.8 | 0.100 |

This should be attributed to the fact that with increasing salt concentration, although the number of charge carriers increased, ion pairs and/or ion aggregations also formed in the system. The former was attributed to an increase of conductivity, but the latter led to a decrease of conductivity. The former effect was dominant and enhanced the conductivity of sample at lower salt concentrations, whereas the latter effect predominated and decreased the conductivity at higher salt concentrations. Thereby, in the whole range of salt content, there existed a maximum of ionic conductivity, which was in agreement with the results of other similar systems.[21]

Figure 7 also reveals that the ionic conductivity of all samples increased with increasing temperature up to 80°C, however, when the temperature was over 80°C, the ionic conductivity remained constant or decreased. Plots of log $\sigma$ versus reciprocal temperature showed nonlinear curves, and this suggested that temperature dependence of ionic conductivity did not follow the Arrhenius equation.

This non-Arrhenius-type temperature dependence of ionic conductivity implies that ion transport occurred mainly in the noncrystalline regions of the polymer complex and was greatly associated with the motions of polymer chains.[22,23] With increasing the temperature, the motions of the polymer chains increased, and the free volume of system was enhanced, which favored ion transport. Therefore, in the temperature range from room temperature to 80°C, ionic conductivity was enhanced with increasing temperature. In addition, there was microseparated structure in polyether PU, and the compatibility between hard and soft segments also
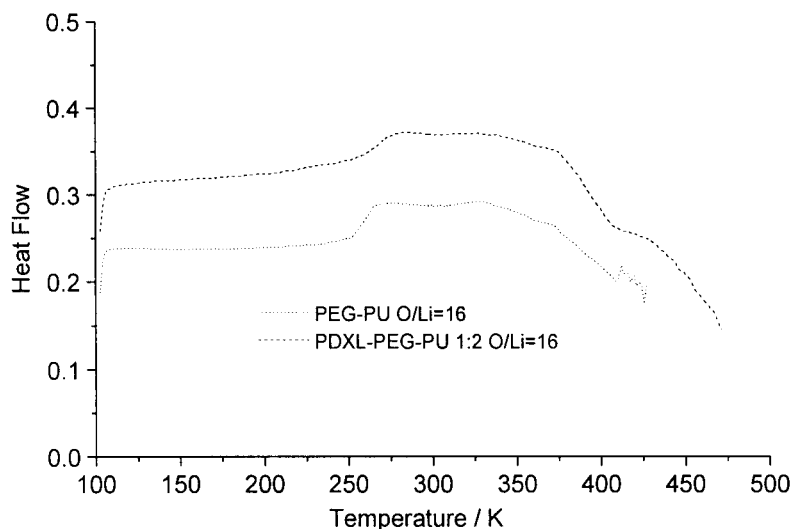


**Figure 5**   DSC thermograms of the PEG–PU/LiClO$_4$ and PDXL–PEG–PU/LiClO$_4$ samples.
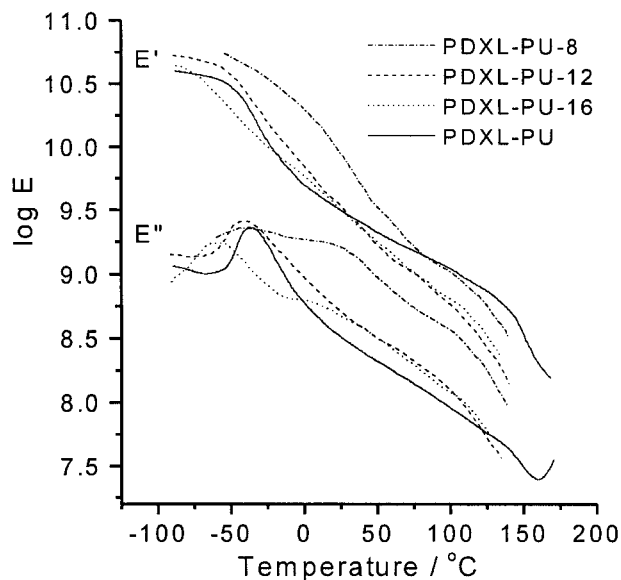
**Figure 6** Dynamic mechanical thermal analysis spectra of the PDXL–PU and PDXL–PU/LiClO$_4$ series.

had a great effect on ionic conductive properties. The increase of the number of hard segments entering domains of soft segments restricted chain motions of soft segments, which led to a decrease in ionic conductivity. From dynamic mechanical analysis results mentioned previously, it was found that all complexes became softer at about 70–80°C. This suggests that the domains of the hard segments became disassociated and part of the hard segments entered domains of soft segments around 70–80°C. The negative effect of the dissociation of hard do-
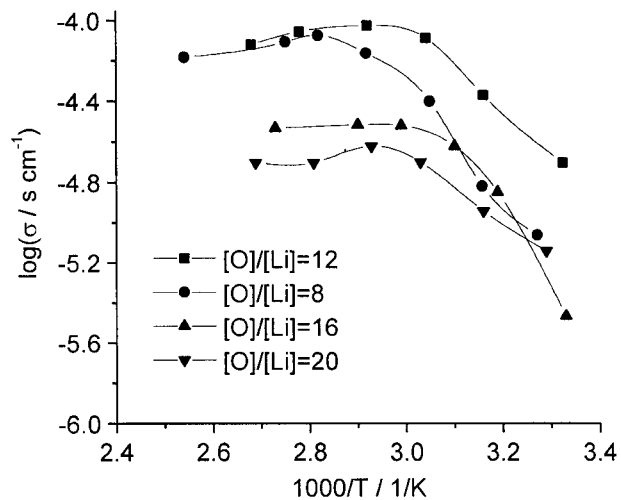


**Figure 7** Temperature dependence of ionic conductivity for the PDXL–PU/LiClO$_4$ series.
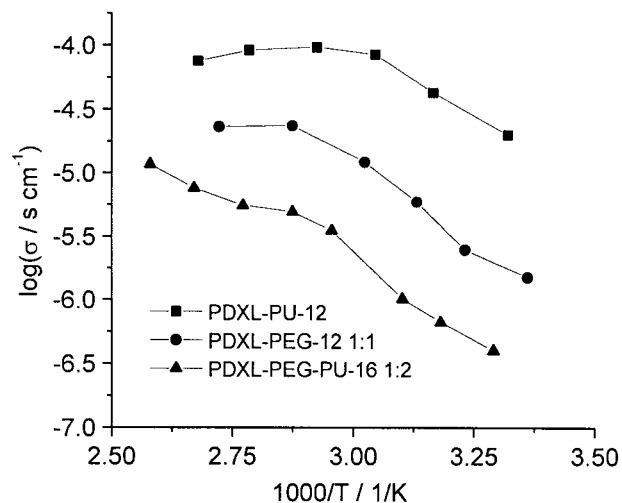


**Figure 8** Temperature dependence of ionic conductivity for the PDXL–PEG–PU/LiClO$_4$ series.

mains on chain motions could counteract and even exceed the positive effect of temperature on chain motions over a certain temperature range. Therefore, when the temperature was above 80°C, the ionic conductivity of samples remained constant or decreased with increasing temperature.

As illustrated in Figure 8, the relationship between ionic conductivity and the temperature of the sample with PDXL : PEG 1 : 1 was similar to that of the PDXL–PU/LiClO$_4$ series. However, the conductivity behavior of the sample with PDXL : PEG 1 : 2 was apparently different from that of the PDXL–PU/LiClO$_4$ series, and the ionic conductivity of the sample increased with increasing temperature. This suggests that effect of the hard-segment domain disassociation on the motions of PEG chains was weaker than that of the temperature on the motions of PEG chains. In addition, the ionic conductivities of samples with PEG as part of the soft segment were lower than that with only PDXL as a soft segment over the whole temperature range investigated, which was consistent with the results of IR analysis and DSC analysis mentioned previously. It could be assumed that the incorporation of a PEG soft segment improved the compatibility between the soft and hard segments and hindered the motions of soft-segment chains, which eventually led to a decrease in ionic conductivity. Figure 8 also reveals that the conductivity behavior of samples with PEG as part of the soft segment did not obey the Arrhenius equation.

## CONCLUSIONS

In summary, FTIR, DSC, dynamic mechanical analysis, and complex impedance analysis were used to investigate thermal transitions, structure, and conductivity in a series of PU-based electrolytes with different polyether soft segments. It was found that the structure of the soft segment had significant influence on the $T_g$ and ionic conductivity of the PU-based electrolytes studied. Results show that the soft segment of PDXL–PU possessed a high ether density and exhibited good flexibility and a low $T_g$ so that PDXL–PU might be a promising host polymer in the field of SPEs.

LiClO$_4$ could be dissolved well in the soft segment of PDXL–PU, and when the value of [O]/[Li] was 12, the highest ionic conductivity of about $2 \times 10^{-5}$ S/cm could be obtained for PDXL–PU/LiClO$_4$ complexes at room temperature. The incorporation of a PEG soft segment into the system improved the compatibility between hard and soft segments. The PDXL–PEG–PU/LiClO$_4$ system had a higher $T_g$ and a lower ionic conductivity than the PDXL–PU/LiClO$_4$ system. The conductivity behavior of the PU-based electrolytes did not follow the Arrhenius equation.

## REFERENCES

1. Wright, P. V. Br Polym 1975, 7, 319.
2. Xu, H. S.; Yang, C. Z. J Polym Sci Part B: Polym Phys 1995, 33, 745.
3. Wang, L.; Yang, B.; Wang, X. L.; Tang, X. Z. J Appl Polym Sci 1999, 71, 1711.
4. Wang, X. L.; Li, H.; Tang, X. Z.; Chang, F. C. J Polym Sci Part B: Polym Phys 1999, 37, 837.
5. Mitsuhiro, S.; Takayuki, K. Eur Polym J 2000, 36, 485.
6. Appetecchi, G. B.; Passerini, S. Electrochim Acta 2000, 45, 2139.
7. Sekhon, S. S.; Gurjinder, S.; Agnihotry, S. A.; Chandra, S. Solid State Ionics 1995, 80, 37.
8. Whang, W. T.; Yang, L. H.; Fan, Y. W. J Appl Polym Sci 1994, 54, 923.
9. Wang, Q.; Gao, J. Polym Mater Sci Eng (Chinese) 1996, 12, 123.
10. Liu, C. S.; Guo, J. S.; Xie, H. Q. Chem J Chin Univ (Chinese) 1994, 15, 1715.
11. Reiche, A.; Sandner, R.; Weinkauf, A.; Sandner, B.; Fleischer, G.; Rittig, F. Polymer 2000, 41, 3821.
12. Peng, Z. L.; Itoh, Y.; Li, S. Q.; Wang, S. J Appl Phys Mater Sci Proc 1996, 63, 267.
13. Moon, S. I.; Lee, C. R.; Jin, B. S.; Min, K. E.; Kim, W. S. J Power Sources 2000, 87, 223.
14. Alamgir, M.; Moulton, R. D.; Abraham, K. M. Electrochim Acta 1991, 36, 14.
15. Foots, J. S.; Erker, S. M. J Electrochem Soc 1987, 34, 122.
16. Ferry, A.; Jacobsson, P.; Heumen, J. D.; Stevens, J. R. Polymer 1996, 37, 737.
17. Wei, X.; Yu, X. H. J Polym Sci Part B: Polym Phys 1997, 35, 225.
18. Rebitaille, C. D.; Fauteux, D. Electrochem Soc 1980, 133, 315.
19. Bruce, P. G.; Krok, F.; Vincent, C. A. Solid State Ionics 1988, 27, 81.
20. Golodnitsky, D.; Peled, E. Electrochim Acta 2000, 45, 1431.
21. Xiong, J.; Zhang, Y. X.; Wang, F. S. Acta Polym Sinica (Chinese) 1991, 1, 7.
22. Zhang, S. S.; Liu, Q. G.; Yang, L. L. Acta Polym Sinica (Chinese) 1993, 3, 366.
23. Sunghoe, Y.; Kimio, I.; William, J. M.; Shaw, L. H. Macromolecules 1995, 28, 5063.